

AD-A145 835

ON THE CAUSE OF X-LINE FORMATION IN THE NEAR-EARTH  
PLASMA SHEET: RESULTS O. (U) RICE UNIV HOUSTON TX DEPT  
OF SPACE PHYSICS AND ASRRONOMY G M ERICKSON 24 APR 84  
SCIENTIFIC-1 AFGL-TR-84-8134

1/1

UNCLASSIFIED

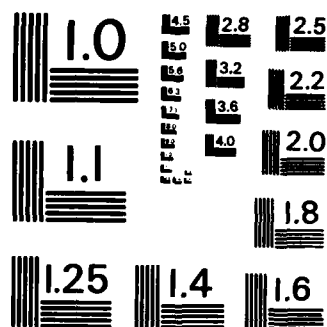
F/G 4/2

NL

END

FILMED

ORC



MICROCOPY RESOLUTION TEST CHART  
NATIONAL BUREAU OF STANDARDS-1963-A

AFGL-TR-84-0134

12

ON THE CAUSE OF X-LINE FORMATION IN THE  
NEAR-EARTH PLASMA SHEET: RESULTS OF ADIABATIC  
CONVECTION OF PLASMA-SHEET-PLASMA

G. M. Erickson

Department of Space Physics and Astronomy  
Rice University  
P.O. Box 1892, Houston, TX 77251

Scientific Report No. 1

24 April 1984

Approved for public release; distribution unlimited

AIR FORCE GEOPHYSICS LABORATORY  
AIR FORCE SYSTEMS COMMAND  
UNITED STATES AIR FORCE  
HANSCOM AFB, MASSACHUSETTS 01731

DTIC  
ELECTE  
SEP 21 1984  
B7

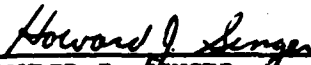
9 1 09 21 010

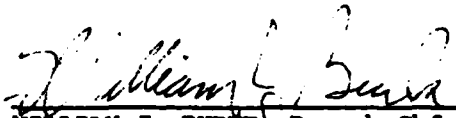
AD-A145 835

DTIC FILE COPY

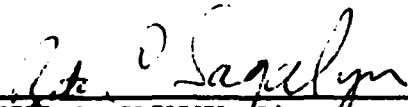
This report has been reviewed by the ESD Public Affairs Office (PA) and is releasable to the National Technical Information Services (NTIS).

"This technical report has been reviewed and is approved for publication"

  
HOWARD J. SLINGER  
Contract Manager

  
WILLIAM J. BURKE, Branch Chf  
Plasmas & Fields Branch  
Space Physics Division

FOR THE COMMANDER

  
RITA C. SAGALYN, Director  
Space Physics Division

Qualified requestors may obtain additional copies from the Defense Technical Information Center. All others should apply to the National Technical Information Service.

If your address has changed, or if you wish to be removed from the mailing list, or if the addressee is no longer employed by your organization, please notify AFGL/DAA, Hanscom AFB, MA 01731. This will assist us in maintaining a current mailing list.

Unclassified

SECURITY CLASSIFICATION OF THIS PAGE (When Data Entered)

REPORT DOCUMENTATION PAGE		READ INSTRUCTIONS BEFORE COMPLETING FORM
1. REPORT NUMBER AFGL-TR-84-0134	2. GOVT ACCESSION NO. AD-A145835	3. RECIPIENT'S CATALOG NUMBER
4. TITLE (and Subtitle) On the Cause of X-Line Formation in the Near-Earth Plasma Sheet: Results of Adiabatic Convection of Plasma-Sheet-Plasma		5. TYPE OF REPORT & PERIOD COVERED Scientific Report No. 1
		6. PERFORMING ORG. REPORT NUMBER
7. AUTHOR(s) G. M. Erickson		8. CONTRACT OR GRANT NUMBER(s) F19628-83-K-0016
9. PERFORMING ORGANIZATION NAME AND ADDRESS Department of Space Physics and Astronomy Rice University, P.O. Box 1892 Houston, TX 77251		10. PROGRAM ELEMENT, PROJECT, TASK AREA & WORK UNIT NUMBERS 61102F 2311G2FE
11. CONTROLLING OFFICE NAME AND ADDRESS U. S. Air Force Geophysics Laboratory Hanscom AFB Massachusetts 01731 Contract Monitor: Dr. Howard J. Singer /PHG		12. REPORT DATE April 24, 1984
		13. NUMBER OF PAGES 25
14. MONITORING AGENCY NAME & ADDRESS (if different from Controlling Office)		15. SECURITY CLASS. (of this report) Unclassified
		15a. DECLASSIFICATION/DOWNGRADING SCHEDULE
16. DISTRIBUTION STATEMENT (of this Report) Approved for public release; distribution unlimited		
17. DISTRIBUTION STATEMENT (of the abstract entered in Block 20, if different from Report)		
18. SUPPLEMENTARY NOTES		
19. KEY WORDS (Continue on reverse side if necessary and identify by block number) Convection Magnetosphere Magnetic field Plasma sheet Substorm		
20. ABSTRACT (Continue on reverse side if necessary and identify by block number) Self-consistent, static-equilibrium solutions are presented for two-dimensional magnetospheric-magnetic-field configurations with isotropic thermal pressure. These solutions include a dipole field and are not restricted to the asymptotic theory. Adiabatic convection of plasma sheet flux tubes is modeled as a series of static-equilibrium solutions in which flux tubes conserve their $PV^{\gamma}$ as they convect, which resulted in time dependent magnetospheric		

Unclassified

SECURITY CLASSIFICATION OF THIS PAGE(When Data Entered)

from review  
Y 2002  
configurations. Specifically, it is found that a deep minimum in the equatorial  $B_z$  develops in the inner plasma sheet, thereby causing the magnetic-field configuration to become more stretched and tail-like in time. These results suggest X-line formation in the inner plasma sheet as a consequence of lossless, adiabatic convection of plasma sheet flux tubes.

Unclassified

SECURITY CLASSIFICATION OF THIS PAGE(When Data Entered)

Additional Information:

(a) Scientists and Engineers Who Contributed to the Research:

G. M. Erickson

G.-H. Voigt

R. A. Wolf

(b) Previous and Related Contracts:

F19628-80-C-0009

F19628-78-C-0078

F19628-77-C-0005

(c) Other Contract-Supported Publications:

R. W. Spiro and R. A. Wolf, "Electrodynamics of Convection in the Inner Magnetosphere," in Magnetospheric Currents, Geophysical Monograph Volume 28, ed. by T. A. Potemra, Am. Geophys. Union, Washington, D. C., p. 247, 1983.

J. L. Karty, R. A. Wolf, and R. W. Spiro, "Region One Birkeland Currents Connecting to Sunward Convecting Flux Tubes," in Magnetospheric Currents, Geophysical Monograph Volume 28, ed. by T. A. Potemra, Am. Geophys. Union, Washington, D.C., p. 269, 1983

DTIC  
ELECTE  
SEP 21 1984  
B



Accession For	
NTIS GRA&I	<input checked="checked" type="checkbox"/>
DTIC TAB	<input type="checkbox"/>
Unannounced	<input type="checkbox"/>
Justification	
By	
Distribution/	
Availability Codes	
Dist	Avail and/or Special
A-1	

ON THE CAUSE OF X-LINE FORMATION IN THE NEAR-EARTH PLASMA SHEET:

RESULTS OF ADIABATIC CONVECTION OF PLASMA-SHEET PLASMA

G. M. Erickson

Department of Space Physics and Astronomy

Rice University, Houston, TX 77251

Abstract. Self-consistent, static-equilibrium solutions are presented for two-dimensional magnetospheric-magnetic-field configurations with isotropic thermal pressure. These solutions include a dipole field and are not restricted to the asymptotic theory. Adiabatic convection of plasma sheet flux tubes is modeled as a series of static-equilibrium solutions in which flux tubes conserve their  $PV^\gamma$  as they convect, which resulted in time dependent magnetospheric configurations. Specifically, it is found that a deep minimum in the equatorial  $B_z$  develops in the inner plasma sheet, thereby causing the magnetic-field configuration to become more stretched and tail-like in time. These results suggest X-line formation in the inner plasma sheet as a consequence of lossless, adiabatic convection of plasma sheet flux tubes.



## Introduction

X-line formation is now regarded as one of the primary candidates for the basic physical process to account for the observed energy dissipation associated with magnetospheric substorms. It is clear that changes in the solar wind can trigger magnetospheric substorms [see, e.g., Akasofu, 1980]. However, it is not clear that magnetospheric substorms are always associated with specific changes in the solar wind. For this reason a substorm mechanism which does not necessarily require an external trigger for X-line formation is attractive. Schindler [1974] offered the following scenario for the substorm mechanism. During the substorm growth phase, free energy is accumulated in the tail, and the tail becomes more and more unstable to perturbations that try to create neutral lines. The presence of a normal magnetic field component in the current sheet inhibits the instability. But when the plasma-sheet becomes sufficiently thin and/or the normal magnetic field component becomes sufficiently small, some breakup mechanism, such as the ion-tearing mode, becomes operative leading to X-line formation and substorm onset [see also Nishida and Nagayama, 1973; Russell and McPherron, 1973; Hones, 1977]. Erickson and Wolf [1980] have presented the argument that approximately lossless, adiabatic, earthward convection of plasma-sheet plasma on closed field lines is necessarily time dependent. They hypothesize that if earthward convection occurs in the tail, even if solar wind conditions were steady, magnetotail field lines would become more and more stretched and tail-like in time resembling the growth phase scenario above. Schindler and Birn [1982] and Birn and Schindler [1983] have self-consistently modeled the quasi-static evolution of tail-like configurations within the framework of the asymptotic theory. They found that in the absence of unrealistic plasma loss, earthward convection is time dependent and drives the tail toward instability.

As discussed by Erickson and Wolf [1980] it is the presence of the earth's dipole field which prevents approximately lossless, adiabatic convection of plasma-sheet flux tubes from proceeding in a time-independent manner. Specifically, it is the fact that plasma cannot expand very far along a line of force in the presence of a dipole field which causes the tail configuration to become more stretched and tail-like as convection proceeds. The asymptotic theory excludes some  $(\vec{B} \cdot \nabla) \vec{B}$  magnetic tension terms in the force balance of the system and, therefore, cannot accurately represent the earth's

dipole field and its critical role as the endpoint of plasma-sheet flux tubes. In this paper, preliminary results are presented of self-consistent modeling of quasi-static convection of plasma-sheet flux tubes in two dimensions. These models include a dipole field and are not restricted to the asymptotic theory. The results of this modeling confirm the results of the previous efforts mentioned above. Also, the results lend support to the Schindler [1974] growth phase scenario, although they do not exclude the possibility of other substorm scenarios [e.g., Coroniti and Kennel, 1972; Akasofu, 1980; Atkinson, 1980].

### Quasi-Static Convection

To model convection of plasma-sheet flux tubes we make the following assumptions: (1) plasma-sheet ions are in bounce equilibrium, (2) thermal plasma pressure is isotropic, (3) inertial forces are small compared to pressure gradients, and (4) convection is lossless. Under these assumptions we seek static-equilibrium solutions of the momentum equation and Maxwell's equations,

$$\vec{J} \times \vec{B} = \nabla P \quad (1)$$

$$\vec{J} = \frac{1}{\mu_0} \nabla \times \vec{B}, \quad (2)$$

and

$$\nabla \cdot \vec{B} = 0. \quad (3)$$

In two dimensions, the magnetic vector potential is  $\vec{A} = A\hat{e}_y$  (GSM coordinates in units of earth radii are used throughout) with  $B_x = -\partial A/\partial z$ ,  $B_z = \partial A/\partial x$ , and (1)-(3) are rewritten as

$$\nabla^2 A = -\mu_0 \frac{dP(A)}{dA} - m \frac{\partial}{\partial x} \delta(x)\delta(z), \quad (4)$$

with

$$P, A = \text{constant along field line.}$$

In (4), the delta function represents the dipole source. Numerical solutions of (4) are obtained on a grid displaced from the origin, and  $A$  is decomposed into its dipole,  $A_d$ , and plasma current source,  $A_j$ , parts. Hence, we actually find solutions of

$$\nabla^2 A_j = -\mu_0 \frac{dP(A)}{dA}. \quad (5)$$

Adjustable parameters of these models include the equatorial plasma pressure, the thickness of the plasma-sheet, and the location of the magnetopause.

By the frozen-in-flux theorem and the fact that in two dimensions both  $P$  and  $A$  are constant along a magnetic field line, we can use  $A$  to tag the plasma as it convects. Also, under the assumptions, the plasma convects so as to keep its  $PV^\gamma$  constant, where  $\gamma$  is the adiabatic index (which we chose to be 2), and

$$V = \int_{f\ell} ds/B \quad (6)$$

is the volume of a flux tube of unit magnetic flux. Thus, convection is modeled as a time-sequence of static-equilibrium solutions of (5) such that each solution shares the same  $PV^\gamma(A)$ . That is, we require that

$$PV^\gamma(A) = \text{independent of time.} \quad (7)$$

## Results

Some examples of self-consistent, two-dimensional magnetospheric-magnetic-field configurations are shown in Figure 1 for different pressure distributions, plasma-sheet heights, and magnetopause locations. Figures 2-5 show the equatorial pressure distribution, the equatorial magnetic field,  $PV^2(x)$ , and  $PV^2(A)$ , respectively, for these models. Note that in order for approximately lossless, adiabatic convection to occur in some region of the tail in a time-independent manner,  $PV^\gamma(x)$  would have to be constant in that region. However, for static-equilibrium configurations that satisfy (1) and include a dipole field,  $PV^\gamma(x)$  (for  $\gamma > 5/3$ ) is not constant but increases with distance down tail. Thus, as earthward convection proceeds, flux tubes entering some region

would have a larger particle content than did their predecessors in the region. Conditions (1) and (7) would then require that the magnetospheric configuration vary in time.

Starting with some self-consistent solution of (1) or (5) at  $t = 0$ , an electric field  $E_{mp}(t)$  is imposed at the magnetopause allowing magnetic flux to enter the magnetopause and forcing earthward convection of plasma-sheet flux tubes. In practice, the value of  $A$  at the magnetopause,  $A_{mp}$ , is changed, the equatorial plasma pressure is adjusted, and new solutions of (5) are obtained until (5) and (7) are satisfied simultaneously. Thus a time sequence of static-equilibrium solutions of (1)-(3) is constructed with time parameterized by the value of  $A_{mp}$ . Forcing Models A and B to convect in this manner resulted in Models A' and B' shown in Figures 6 and 9. In Model B' modeling was performed only out to  $x = -60.5 R_E$  where the height of the plasma-sheet was chosen so that  $PV^2(x)$  had zero slope there at  $t = 0$ . Beyond  $x = -60.5 R_E$ ,  $PV^2$  was assumed constant. For  $t > 0$ , the height of the plasma-sheet was chosen such that the amount of magnetic flux contained between the top of the plasma-sheet and the magnetopause was constant in time. For quiet times and a constant electric field of  $10^{-4}$  V/m at the magnetopause, the three "snapshots" of Figures 6 and 9 for  $A_{mp} = 0, -12$ , and  $-22$  correspond to  $t = 0, 1.5$ , and  $2.7$  hrs, respectively. For an electric field of  $5 \times 10^{-4}$  V/m the respective times would be  $t = 0, 0.3$ , and  $0.54$  hrs. The conversion of the other physical quantities from the units used to SI units is given in the Appendix.

As expected, the adiabatic convection of plasma-sheet flux tubes resulted in time-dependent configurations, consistent with the earlier conclusions of Erickson and Wolf [1980] and Schindler and Birn [1982] that steady-state convection is theoretically unlikely in the magnetotail. Being unable to convect in a steady state, the field strength in the lobe increases as flux is piled up, and the configuration becomes more tail-like in time. Figures 7 and 10 show the evolution of the equatorial pressure distribution for Models A' and B'. The drift of plasma around the earth was accounted for by defining the equatorial pressure at the origin to be the maximum pressure of the system for all times. Thus the pressure was allowed to reach this value but not exceed it. Figures 8 and 11 show the evolution of the equatorial magnetic field  $B_e$  for Models A' and B'. Note the minimum in  $B_e$  that develops (and gets deeper with time) near  $-10 R_E$ , corresponding to the stretching of the field in the

near-earth part of the plasma-sheet as higher and higher content flux tubes are convected into the region. Also, the plasma current density has approximately doubled in this region from  $A_{mp} = 0$  to  $A_{mp} = -22$ . It is in this near-earth plasma-sheet region that the tail appears least stable.

Admittedly, the manner in which the drift of plasma around the earth is treated does not seem very realistic. This feature was chosen merely for numerical simplicity and convenience. Condition (7) was strictly enforced tailward of the  $P = \text{constant}$  region, while it was not enforced inside the  $P = \text{constant}$  region. This resulted in a sharp inner edge of the current sheet with current density increasing from zero to its peak value within only a few  $R_E$ . The westward currents in the plasma-sheet contribute a positive  $B_z$  earthward of the peak in the current density. As higher and higher content flux tubes convected into the near-earth part of the plasma-sheet, westward current increased resulting in a local  $B_z$  minimum just earthward of the current density maximum. In a more realistic treatment the drift of plasma out of the noon-midnight meridian plane and around the earth would still occur within only a few  $R_E$ , but the artificial constraint that the pressure not exceed a certain constant value would be removed. In that case a peak in the plasma pressure might develop just tailward of the inner edge of the plasma-sheet. The current,  $-dP/dA$ , would change sign at this peak in a closed-field-line configuration. As higher and higher content flux tubes convect into the region, the westward current tailward of the peak and the eastward current within the inner edge would increase, resulting in a  $B_z$  minimum near the plasma pressure peak. Thus, we would expect that a more realistic treatment would not qualitatively change the results. However, details such as the exact location or width of the  $B_z$  minimum might be different.

A rectangular magnetopause was also chosen for numerical simplicity. Results of the static modeling show that the choice of dayside magnetopause has little effect on the tail configuration. Also, flaring of the tail magnetopause affects the  $PV(A)$  curves in much the same way as the height of the plasma-sheet does. Thus we expect that the general behavior of the convection models presented here will also occur for more realistic magnetopause shapes.

## Summary

The effect of slow, sunward convection in a magnetospheric plasma-sheet has been investigated using computed two-dimensional, force-balanced magnetic field configurations, including the earth's dipole field. The results confirm the earlier conclusions of Erickson and Wolf [1980] and Schindler and Birn [1982] that approximately lossless, adiabatic convection of plasma-sheet flux tubes is a time-dependent process. In this process the magnetotail becomes more stretched and tail-like as convection proceeds, resulting in configurations more unstable to perturbations which try to create neutral lines. The results support the Schindler [1974] growth-phase scenario, although they do not exclude other possibilities. Preliminary results suggest that forcing plasma-sheet plasma to adiabatically convect sunward leads to a buildup of magnetic energy in the magnetotail. A minimum in the equatorial field strength develops in the near-earth part of the plasma-sheet, and that minimum rapidly deepens as convection proceeds, which obviously suggests formation of a near-earth X-line.

## Appendix

The unit of distance used here is  $R_E$  ( $6.38 \times 10^6$  m). The other physical quantities are given in arbitrary units which can be converted to MKS units as follows:

$$P \rightarrow \delta P / (\mu_0 R_E^4),$$

$$A \rightarrow \delta^{1/2} A / R_E,$$

$$B \rightarrow \delta^{1/2} B / R_E^2,$$

$$V \rightarrow V / (\delta^{1/2} R_E^3).$$

Time is parameterized as the value of  $A_{mp}$ , the value of  $A$  on the magnetopause. Given the electric field at the magnetopause,  $E_{mp}(t)$ , time (in seconds) is determined from

$$\int_0^t E_{mp}(t') dt' = -A_{mp}.$$

Acknowledgments. The author is grateful to Michael Heineman and Ken Yates for stimulating conversations.

## References

- Akasofu, S.-I., The solar wind-magnetosphere energy coupling and magnetospheric disturbances, Planet. Space Sci., 28, 495-509, 1980.
- Atkinson, G., The expansive phase of the magnetospheric substorm, in Dynamics of the Magnetosphere, ed. S.-I. Akasofu, pp. 461-481, D. Reidel Publ. Co., Dordrecht, Holland, 1980.
- Behannon, K. W., Mapping of the earth's bow shock and magnetic tail by Explorer 33, J. Geophys. Res., 73, 907-930, 1968.
- Birn, J., and K. Schindler, Self-consistent theory of three-dimensional convection in the geomagnetic tail, J. Geophys. Res., 88, 6969-6980, 1983.
- Coroniti, F. V., and C. F. Kennel, Polarization of the auroral electrojet, J. Geophys. Res., 77, 2835-2850, 1972.
- Erickson, G. M., and R. A. Wolf, Is steady convection possible in the earth's magnetotail?, Geophys. Res. Lett., 7, 897-900, 1980.
- Fuchs, F., and G.-H. Voigt, Self-consistent theory of a magnetospheric B-field model, in Quantitative Modeling of the Magnetospheric Processes, ed. W. P. Olson, pp. 86-95, AGU, Washington, D.C., 1979.
- Hones, E. W., Jr., Substorm processes in the magnetotail: Comments on 'On hot tenuous plasma, fireballs, and boundary layers in the earth's magnetotail' by L. A. Frank, K. L. Ackerson, and R. P. Lepping, J. Geophys. Res., 82, 5633-5640, 1977.
- Nishida, A., and N. Nagayama, Synoptic survey for the neutral line in the magnetotail during the substorm expansion phase, J. Geophys. Res., 78, 3782-3798, 1973.
- Russell, C. T., and R. L. McPherron, The magnetotail and substorms, Space Sci. Rev., 15, 205-266, 1973.
- Schindler, K., A theory of the substorm mechanism, J. Geophys. Res., 79, 2803-2810, 1974.
- Schindler, K., and J. Birn, Self-consistent theory of time-dependent convection in the earth's magnetotail, J. Geophys. Res., 87, 2263-2275, 1982.



## Figure Captions

Fig. 1. Some examples of self-consistent, two-dimensional, magnetospheric-magnetic-field configurations. Tail field lines are shown containing equal amounts of magnetic flux. The amount of magnetic flux passing through the right boundary is the same in each example. (a) Model A. Using the appropriate boundary conditions ( $P$  and  $A$  at the magnetopause,  $P$  in the equatorial plane,  $B_x(z = 0) = 0$ , and one-dimensional force balance at the right boundary) a modified ( $P = \text{constant}$  for  $0 > x > -4.5 R_E$ ) Fuchs-Voigt [1979] model with  $k = 1.54$  is obtained. The Fuchs-Voigt analytic models feature an exponential decline of the physical quantities down the tail. (b) Model B. This model is the same as Model A except that the height of the plasma-sheet (dotted line) is chosen as  $6 R_E$  at  $x = -60.5 R_E$ . (c) Model C. In this model the equatorial pressure declines as  $|x|^{-1.2}$ , based on the observations of Behannon [1968]. (d) Model D. This model has the same equatorial pressure as Model A, but the tail magnetopause is flared ( $5.7^\circ$ ), and the dayside magnetopause is rounded.

Fig. 2. The equatorial pressure profiles for Models A-D. Note that  $dP/dx$  for Models A, B, and D is the same.

Fig. 3. The equatorial magnetic field,  $B_e$ , for Models A-D.

Fig. 4.  $PV^2$  vs.  $x$  for Models A-D. A constant  $PV^2(x)$  is required for steady, lossless, adiabatic convection.

Fig. 5.  $PV^2$  vs.  $A$  for Models A-D. The approach of the top of the plasma-sheet to the equatorial plane implies a neutral line tailward of the right boundary in Model B. When Model B is convected, it is assumed that flux tubes of constant  $PV^2$  enter the right boundary represented by the dashed-line continuation of the  $PV^2(A)$  curve.

Fig. 6. Model A' showing the results of convecting Model A under the constraint that  $PV^2(A)$  remains unchanged (as explained in the text). The two-dimensional magnetic field configuration is shown for  $A_{mp} = 0$  (top panel),  $A_{mp} = -12$  (middle panel), and  $A_{mp} = -22$  (bottom panel). Tail field lines are shown containing equal amounts of magnetic flux. The  $A = 0$  field line is labeled, and the dashed field line is  $A = 30$  for reference.

Fig. 7. The equatorial plasma pressure for Model A' for  $A_{mp} = 0$ ,  $-12$ , and  $-22$ . The end of the  $P = \text{constant}$  region is at  $x = -8.5 R_E$  for  $A_{mp} < -12$ .

Fig. 8. The equatorial magnetic field for Model A' for  $A_{mp} = 0$ ,  $-12$ , and  $-22$ .

Fig. 9. Model B' shows the results of convecting Model B in the same manner as Model A with the additional condition that the total flux contained between the top of the plasma-sheet (dotted line) and the magnetopause is constant. The snapshots shown are displayed in the same manner as Figure 6.

Fig. 10. Same as Figure 7 for Model B'.

Fig. 11. Same as Figure 8 for Model B'.

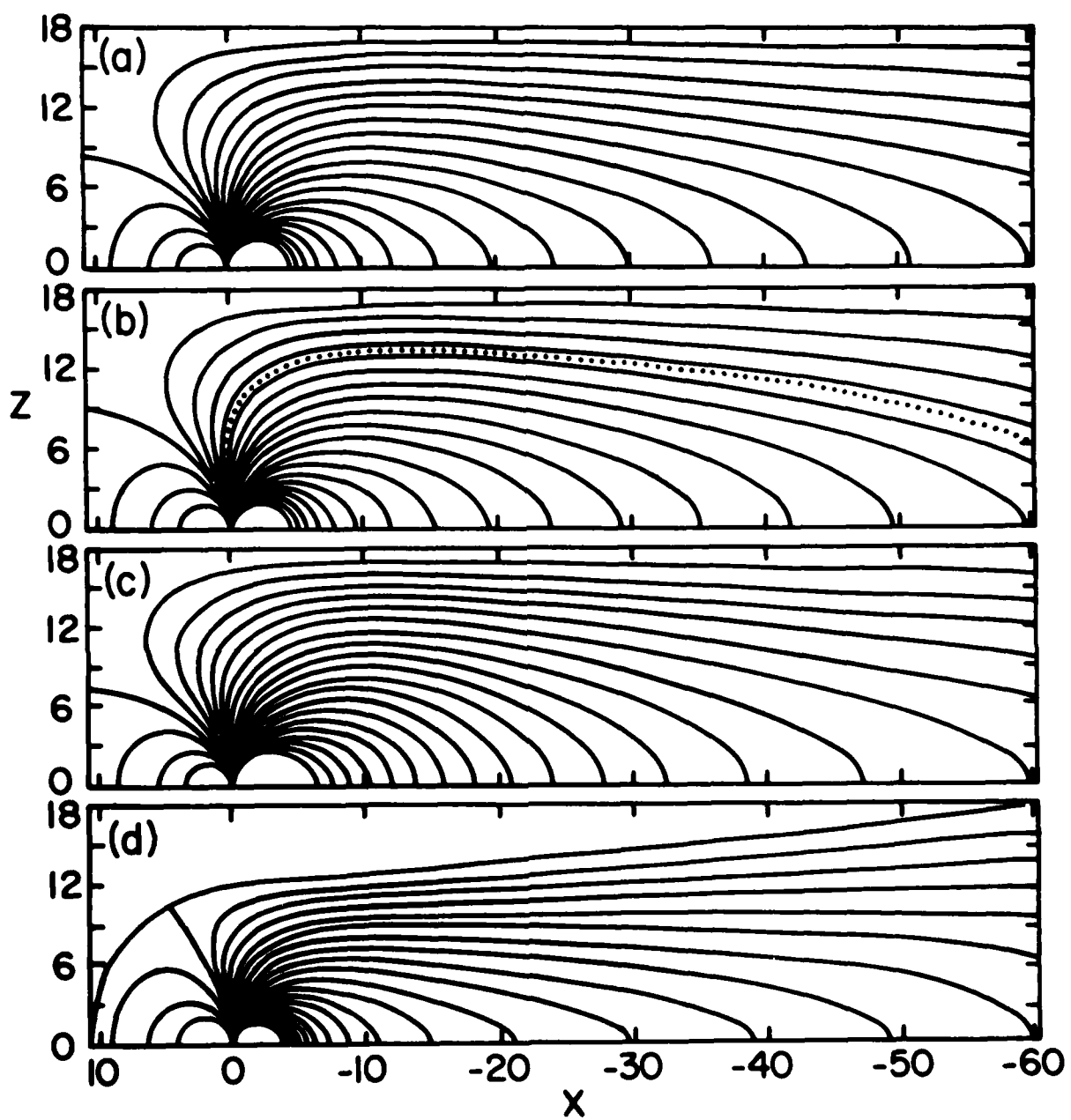


Figure 1

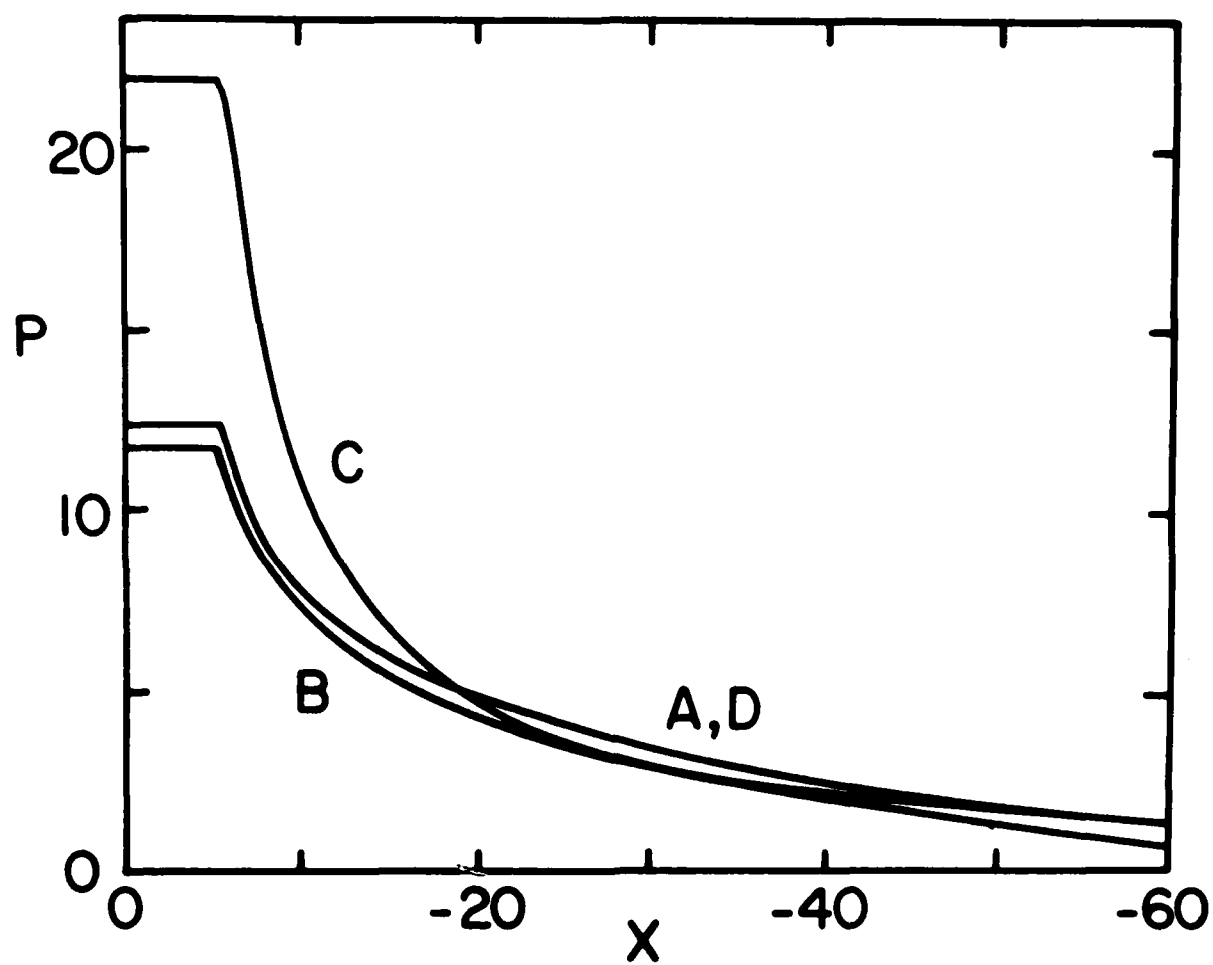


Figure 2

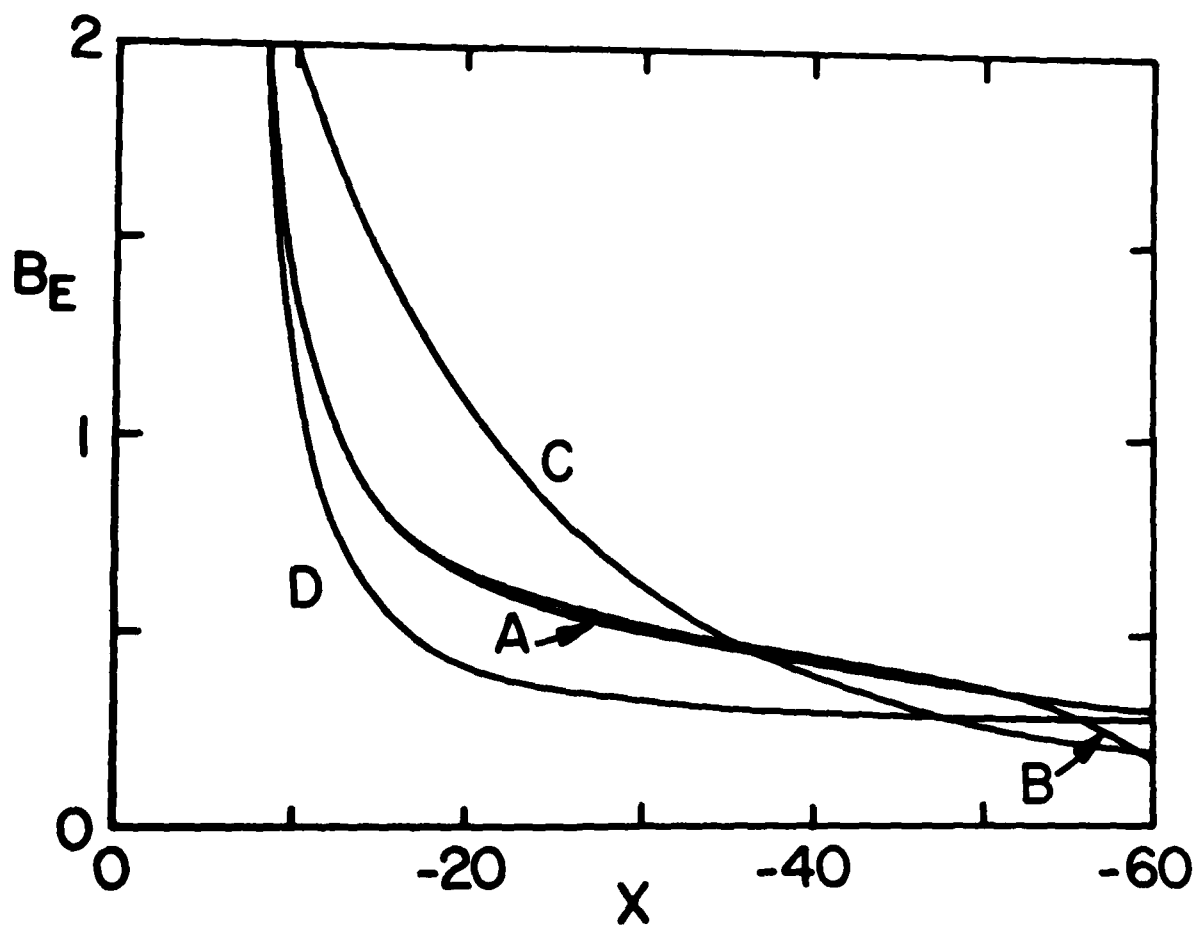


Figure 3

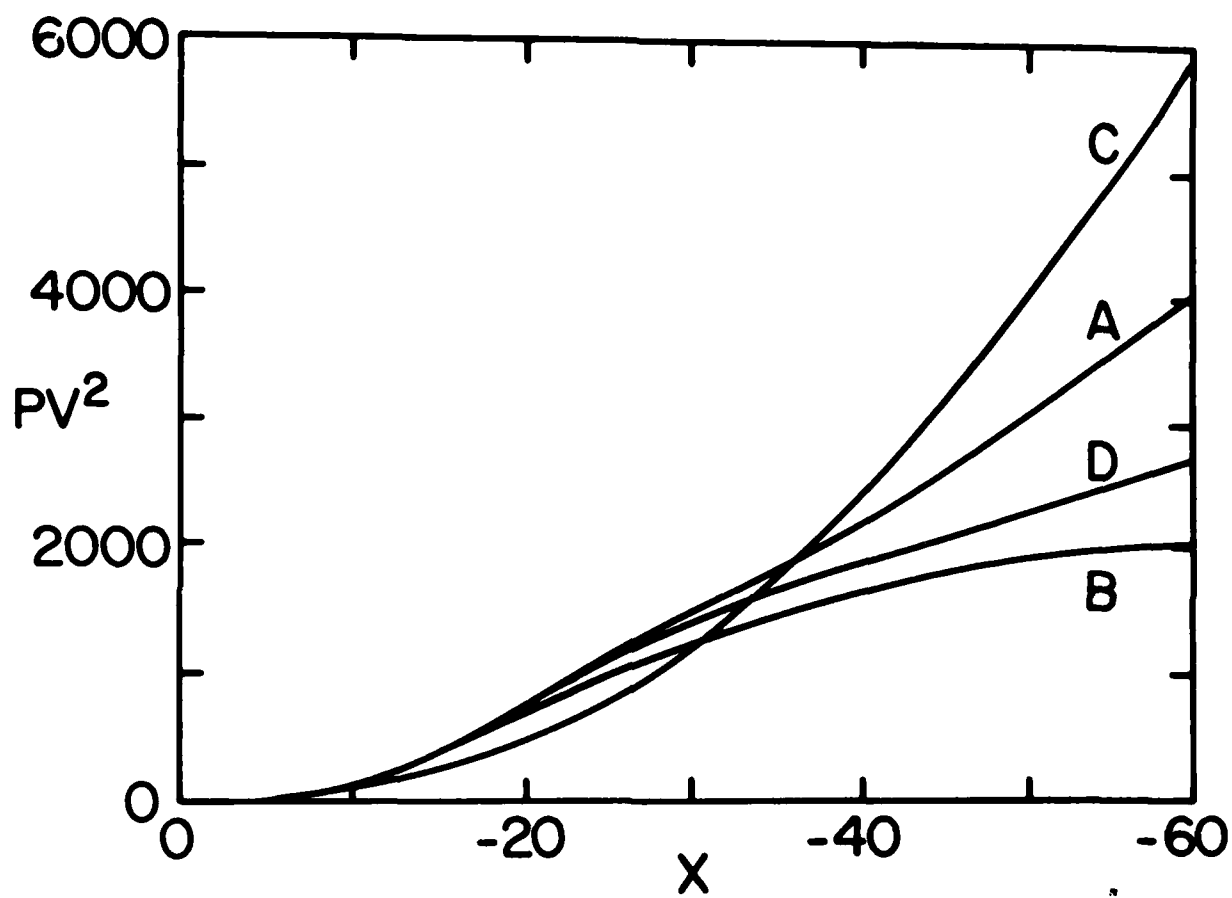


Figure 4

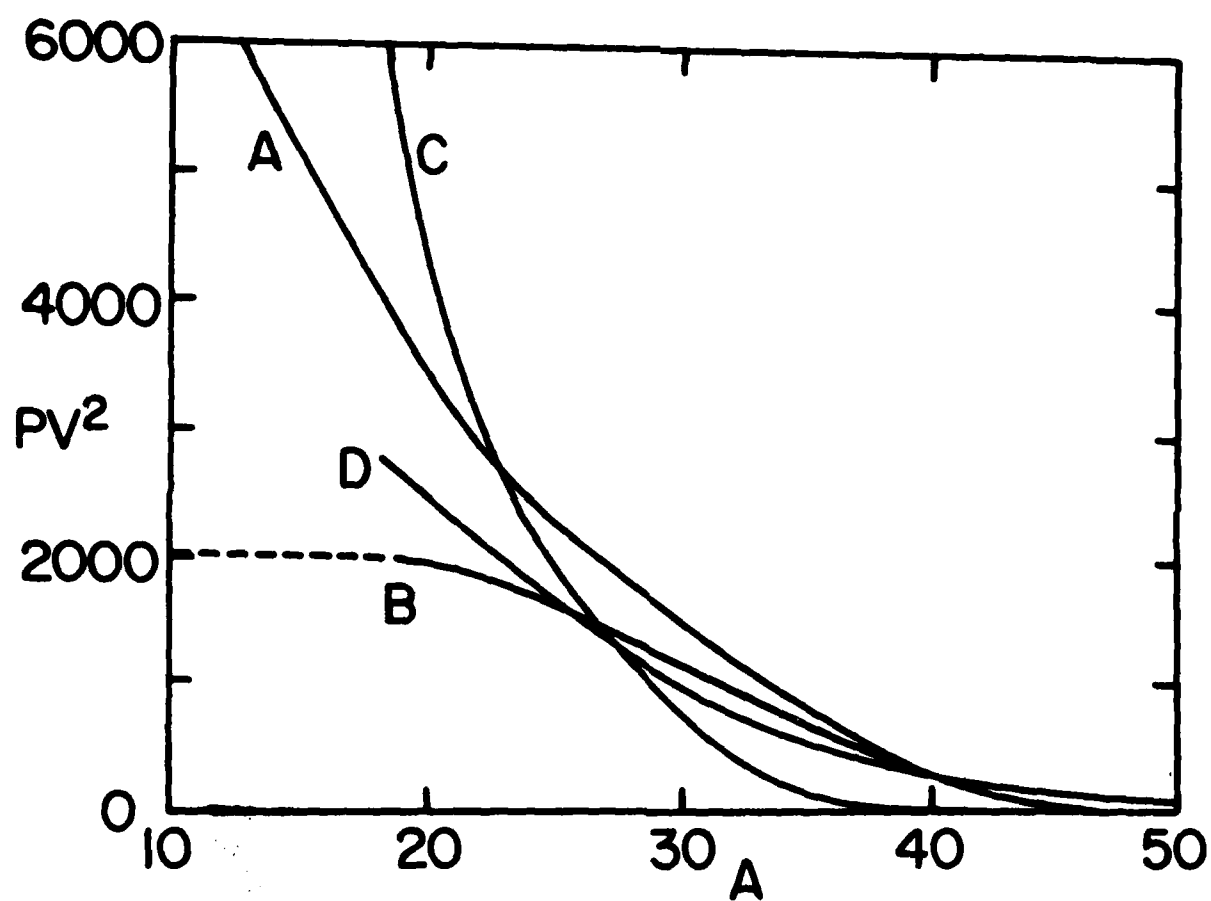


Figure 5

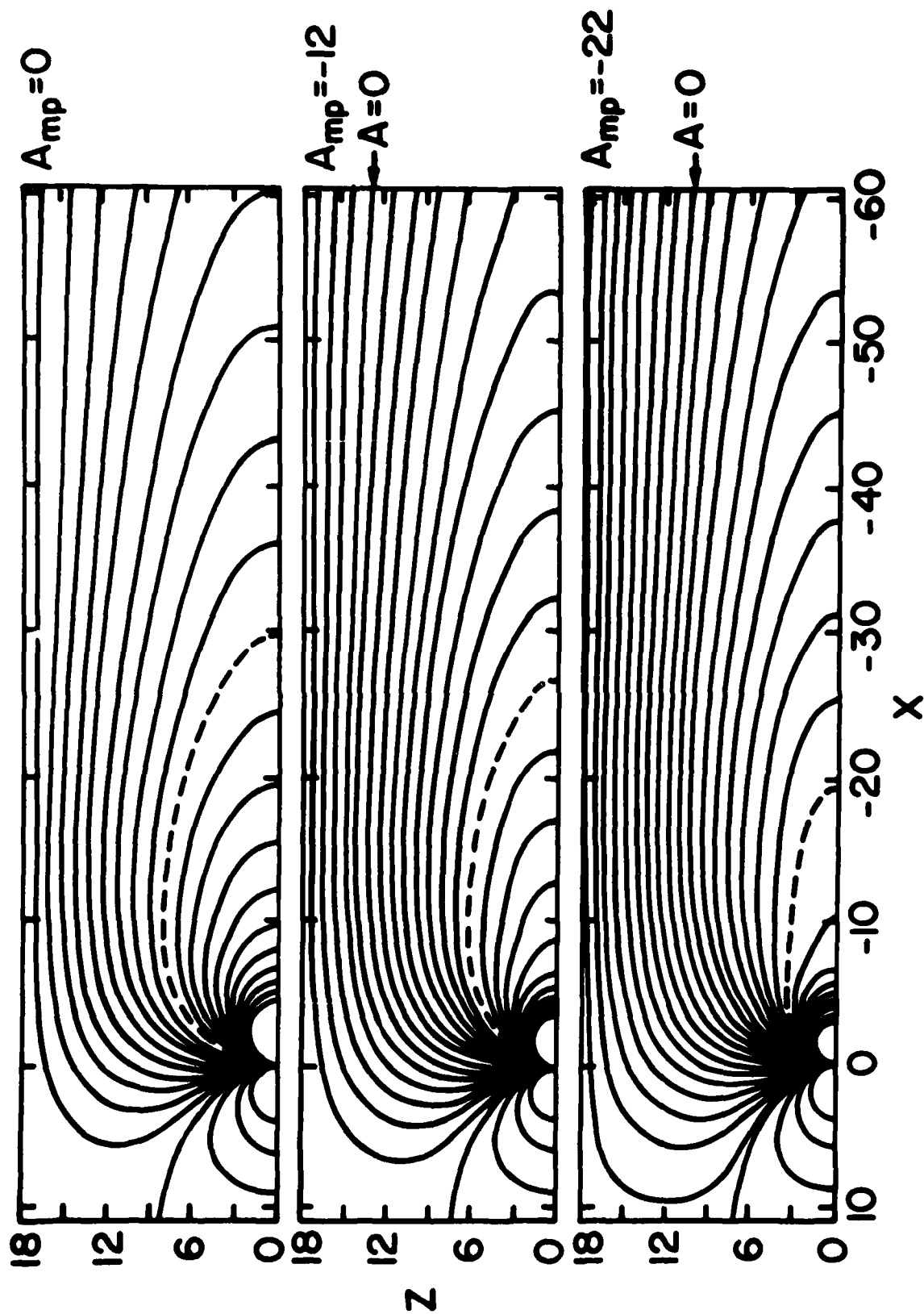


Figure 6



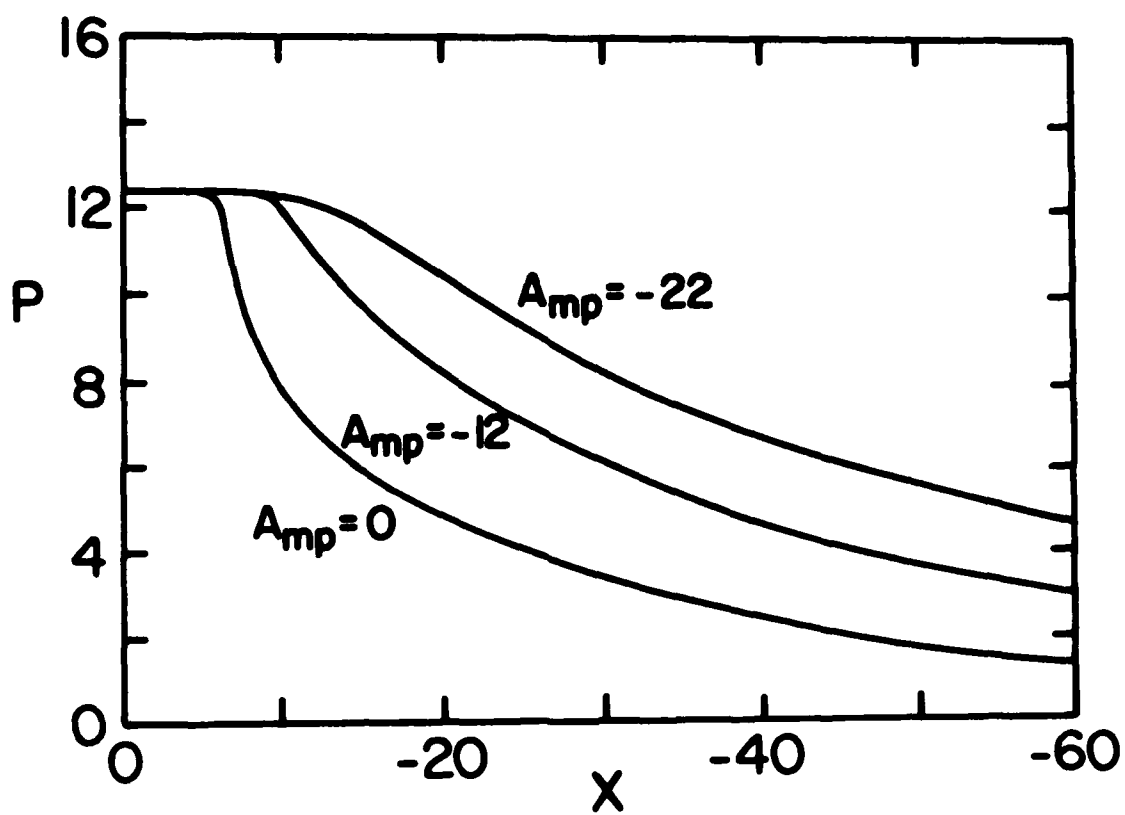


Figure 7

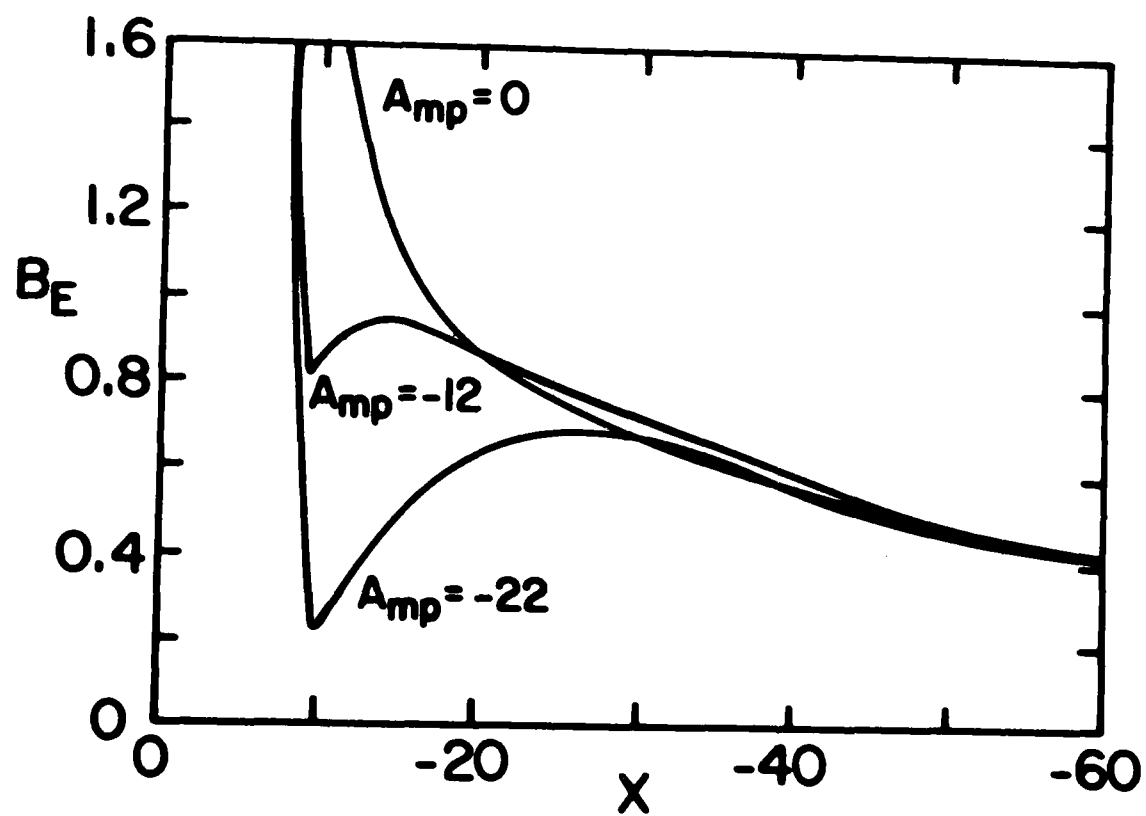


Figure 8

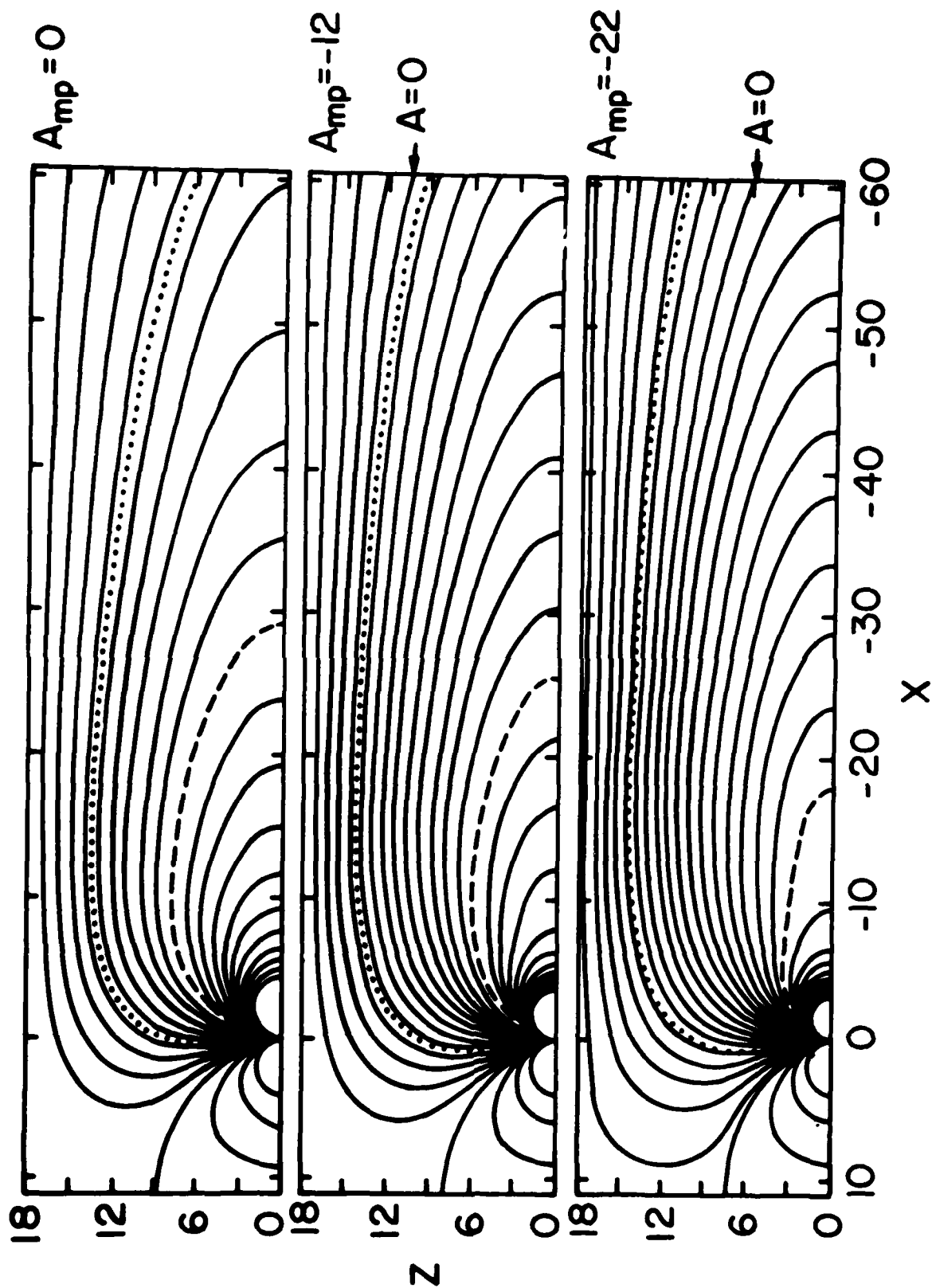


Figure 9

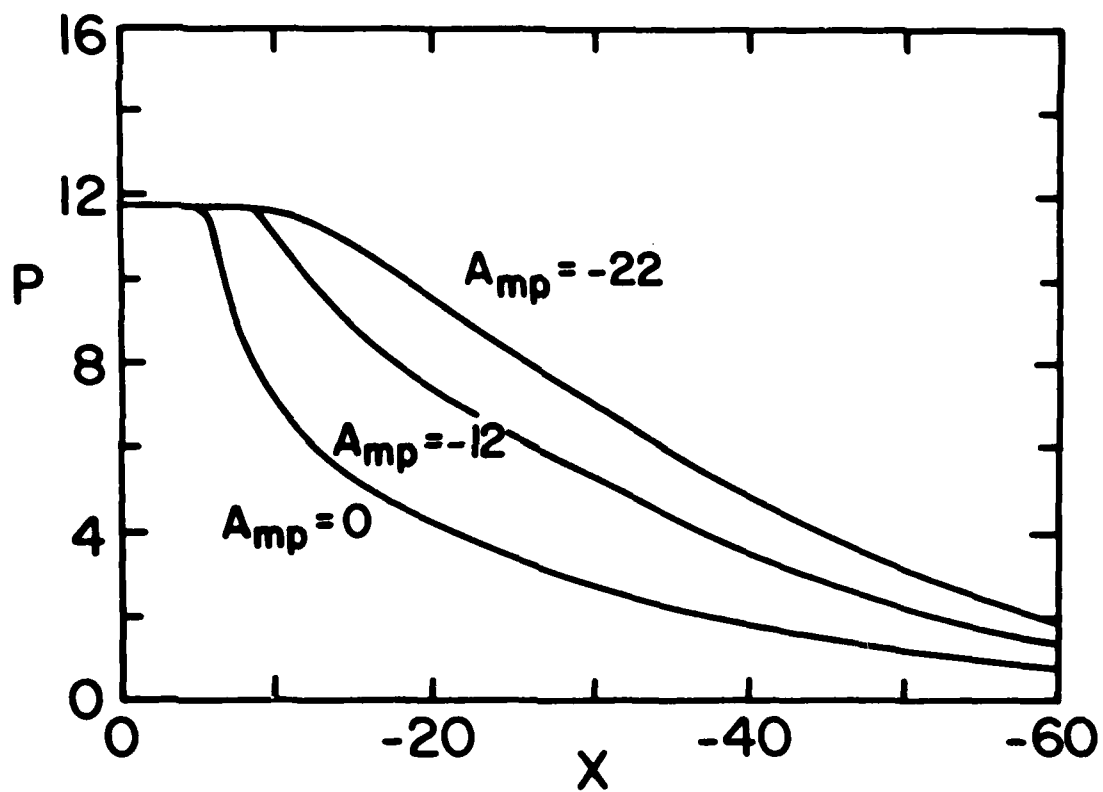


Figure 10

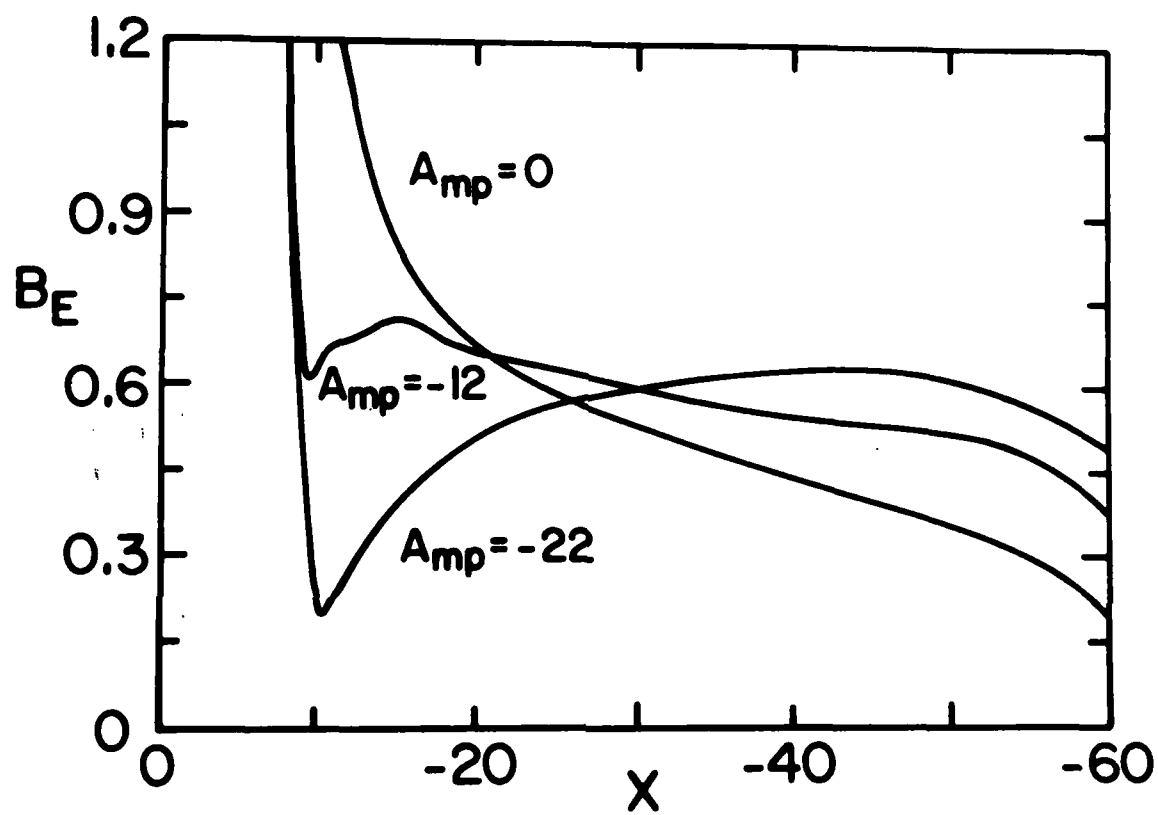


Figure 11

